ENDOR and EPR studies of benzene radical cations in halocarbon matrices: the static Jahn–Teller distortion of the monomer and geometry of the dimer cation. Chem Phys Lett

ARTICLE *in* CHEMICAL PHYSICS LETTERS · JULY 1998

Impact Factor: 1.9 · DOI: 10.1016/S0009-2614(98)00541-7

5 AUTHORS, INCLUDING:

Kenji Komaguchi
Hiroshima University
94 PUBLICATIONS **1,523** CITATIONS
SEE PROFILE

Anders Lund
Linköping University
288 PUBLICATIONS **3,229** CITATIONS
SEE PROFILE

3 July 1998

ELSEVIER

Chemical Physics Letters 290 (1998) 371–378

CHEMICAL PHYSICS LETTERS

ENDOR and EPR studies of benzene radical cations in halocarbon matrices: the static Jahn–Teller distortion of the monomer and geometry of the dimer cation

R.M. Kadam [a], R. Erickson [a], K. Komaguchi [b], M. Shiotani [b], A. Lund [a,*]

[a] *Department of Physics and Measurement Technology, Linköping University, S-58183 Linköping, Sweden*
[b] *Department of Applied Chemistry, Faculty of Engineering, Hiroshima University, Higashi-Hiroshima 739, Japan*

Received 13 February 1998; in final form 30 April 1998

Abstract

ENDOR investigations of the benzene radical cation in a $CFCl_3$ matrix at 30 K gave evidence for a static Jahn–Teller distortion with the unpaired electron density predominantly in the $^2b_{2g}$ orbital. In this distortion the equivalence of the six protons is lost, with the major spin densities on H_1 and H_4. From ENDOR measurements the isotropic and dipolar couplings were accurately measured ($a_{iso} = -25.31$ MHz (H_1 and H_4) and $a_{iso} = -5.43$ MHz (H_2, H_3, H_5 and H_6)) which agree with those reported earlier from EPR measurements and theoretical calculations. $(C_6H_6)_2^{+\cdot}$, formed by warming in $CFCl_3$ at 140 K and initially present in CF_3CCl_3, was characterised with ENDOR and assigned to a π-electron complex. The intermolecular distance was estimated from the measured dipolar hyperfine coupling to be in the range 2–3 Å.

1. Introduction

Electron paramagnetic resonance (EPR) is used extensively to investigate radiation induced defects, electronic structure of radicals, molecular dynamics [1–3] and also to probe the distortions of radicals with an unpaired electron in a degenerate highest occupied molecular orbital (HOMO) undergoing static Jahn–Teller distortions [4–7]. Such distortions have been reported in ethane$^{+\cdot}$, cyclopropane$^{+\cdot}$ and benzene$^{+\cdot}$. Among these, the radical cation of benzene is of fundamental interest due to its simple structure and high symmetry. Iwasaki et al. [7] have stabilised benzene radical cations in a $CFCl_3$ matrix and obtained EPR evidence for the Jahn–Teller distortion at 4.2 K, with the unpaired electron density in the $^2b_{2g}$ orbital. The EPR studies clearly indicated the inequivalence of the six protons caused by this distortion with the major spin density on the C_1 and C_4 carbon atoms resulting in $a_1 = a_4 = -22.96$ MHz and $a_2 = a_3 = a_5 = a_6 = -6.72$ MHz. In addition to this aromatic radical, cations of benzene, naphthalene and biphenyl can be stabilised in halocarbon matrices or adsorbed on an HY molecular sieve, silica gel and on zeolite surfaces [8–14]. The EPR studies of the benzene radical cation adsorbed on the HY molecular sieve at 203 K resulted in spectra characterised by axially symmetric $\boldsymbol{g}$ and $\boldsymbol{A}$ tensors with $g_{\parallel} = 2.00238$, $g_{\perp} = 2.00256$, $A_{\parallel} = -14.00$ MHz and $A_{\perp} = -11.34$ MHz. This suggests rapid

* Corresponding author.

0009-2614/98/$19.00
PII: S0009-2614(98)00541-7

rotation of the benzene cation about the molecular six-fold symmetry axis [8]. The EPR, ENDOR and ESEEM studies of $C_6H_6^{+\cdot}$ and $C_6H_5D^{+\cdot}$ radical cations adsorbed on the HY molecular sieve and silica gel suggested that the $C_6H_6^{+\cdot}$ radical cation undergoes pseudorotation at 3.5 K, whereas in the $C_6H_5D^{+\cdot}$ radical cation on a silica gel a broadening was observed of the quintet hyperfine structure upon lowering the temperature, evidence of the slowing down of the molecular motion to a rigid or semirigid state [9]. In this case, the EPR spectrum with five equivalent protons has changed to one with four equivalent protons with dominant hyperfine structure due to Jahn–Teller distortion with unpaired electron density on a $^2b_{1g}$ orbital.

Though Iwasaki et al. [7] reported Jahn–Teller distortion in the $C_6H_6^{+\cdot}$ radical cation in a $CFCl_3$ matrix, in their investigations the EPR signal arising from two different sets of inequivalent protons were poorly resolved due to the disordered nature of the sample. This might give some error in the hyperfine coupling constants from ESR measurements alone. Furthermore in powder samples, the spectral interpretation of the EPR signal is hampered due to g − and hyperfine anisotropy and inhomogeneous line broadening. In addition to this, EPR resolution is further reduced as the unpaired electron interacts with inequivalent nuclei, thereby increasing the number of EPR transitions. In the present studies we have used the EPR and ENDOR techniques to investigate the Jahn–Teller distortion of the $C_6H_6^{+\cdot}$ radical cations in a $CFCl_3$ matrix. In the Jahn–Teller distortion, the equivalence of the six protons is lost and this would be clearly reflected in the ENDOR spectrum, because of its higher resolution compared to ESR and also due to the simplicity of the ENDOR spectrum as it gives a pair of lines for each set of equivalent protons. We have obtained precise isotropic and dipolar couplings for the distorted benzene radical cation from ENDOR measurements. The results of these investigations are compared to those obtained experimentally [7] and by theoretical calculations of hyperfine coupling constants [15].

In the early studies of dimeric benzene ions, the geometry could not be unambiguously assigned due to the low resolution [16,17]. In this study the species was characterised by solid state ENDOR. From an analysis of the data, a sandwich π-electron complex was inferred with a distance between the rings in the range 2–3 Å. This agrees with the structure predicted by semiempirical molecular orbital calculations [18].

2. Experimental

EPR quartz tubes filled either with $CFCl_3$ or CF_3CCl_3 solvent were immersed in liquid nitrogen. The tubes were connected to a vacuum line and after degassing ~1 mol% benzene was added to the sample. The sample was brought to room temperature and again frozen rapidly to produce a truly polycrystalline sample. The samples were irradiated for 10 min at 77 K using an X-ray source with a tungsten anode operating at 70 kV and 20 mA. EPR and ENDOR experiments were performed on a Bruker ER 200 D spectrometer with an ENDOR attachment. The EPR and ENDOR experiments above 100 K were conducted using a Bruker VT 4111 temperature controller, whereas the ENDOR experiments in the temperature range 4.2–100 K were done with an Oxford ESR900 helium cryostat.

3. Results

Benzene in a $CFCl_3$ matrix has a tendency to form a partly oriented state in which the amount of order/disorder depends on the concentration of benzene and freezing time. The tendency to form partly oriented samples is unique to the $CFCl_3$ matrix and this orientation effect has been previously observed [7]. We have tested the polycrystalline nature of the sample by rotating the sample in a magnetic field. In the samples used in the present investigations, no orientational dependence was observed, indicating the truly polycrystalline nature of the sample.

3.1. EPR results

The EPR spectrum of the $C_6H_6^{+\cdot}$ radical cation in a $CFCl_3$ matrix at 15 K is shown in Fig. 1 along with the simulated spectrum. The hyperfine coupling and *g* tensor data used for EPR and ENDOR simulations are given in Table 1. The spectrum is dominated by three lines separated by ~13.4 G. The intensity of the central line is larger than the binomial intensity

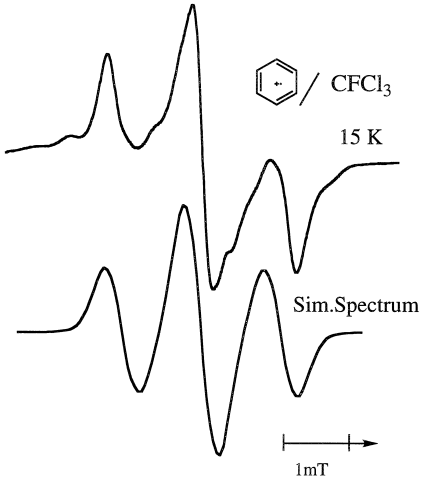

Fig. 1. Comparison of experimental (top) and simulated (bottom) EPR spectra of the polycrystalline benzene radical cation in a $CFCl_3$ matrix at 15 K. The simulation is done by using parameters given in Table 1 and a linewidth of 0.3 mT.

distribution for two equivalent protons, indicating the presence of additional unresolved small hyperfine couplings. The EPR spectrum at 15 K corresponds to a benzene radical cation with the dominant hyperfine coupling from two equivalent protons arising from static Jahn–Teller distortion due to the lowering of the symmetry of $C_6H_6^{+\cdot}$. The spectral lineshape is caused by the hyperfine anisotropy for two different sets of protons. The EPR spectra in the range 77–160 K is shown in Fig. 2. Upon increasing the temperature from 77 to 100 K, the EPR spectrum changes reversibly with respect to the lineshape of the spectrum and also the number of hyperfine components. The changes in the EPR spectra between 77 and 100 K were attributed to the $C_6H_6^{+\cdot}$ cation undergoing rotation about the six-fold axis to average anisotropy in g and A. On warming the sample further it was seen that a new species appeared in the EPR spectrum with more hyperfine components. The new species, with a coupling constant of 2.17 G, was assigned to the benzene dimeric cation $(C_6H_6)_2^{+\cdot}$ from the number of hyperfine components and the hyperfine coupling constant. Beyond 160 K the dimer signal disappeared completely due to the melting of the matrix. The EPR spectrum of the dimeric benzene cation in the CF_3CCl_3 matrix at 50 K is also shown in Fig. 2 along with the simulated spectrum.

3.2. ENDOR results, simulations and line assignment for $C_6H_6^{+\cdot}$

The ENDOR signal of the $C_6H_6^{+\cdot}$ cation in a $CFCl_3$ matrix at 30 K was obtained by saturating the central EPR signal and is shown in Fig. 3. The strong ENDOR line in the region 14 MHz, along with some weak transitions in the region 2–7 MHz is due to the matrix radical. The ENDOR signals outside this region corresponds to principal values of the ring proton hyperfine tensors. Two sets of EN-

Table 1
g and hyperfine tensors (in MHz) used in the EPR and ENDOR simulations of $C_6H_6^{+\cdot}$ in a $CFCl_3$ and $(C_6H_6)_2^{+\cdot}$ in a CF_3CCl_3 matrix at 30 and 110 K, respectively

Tensors	Principal components	Principal value	x	y	z
$C_6H_6^{+\cdot}$	g_x	2.0029	1	0	0
	g_y	2.0029	0	1	0
	g_z	2.0023	0	0	1
A (1 and 4)	A_x	−38.80	1	0	0
	A_y	−11.09	0	1	0
	A_z	−26.01	0	0	1
A (2, 3, 5, 6)	A_x	−8.40	±0.3771	0.9262	0
	A_y	0.00	−0.9262	±0.3771	0
	A_z	−7.90	0	0	1
$(C_6H_6)_2^{+\cdot}$	A_x	−6.72	1	0	0
	A_y	−6.72	0	1	0
	A_z	−4.76	0	0	1

Conversion factor is 1 G = 2.8024 MHz.

DOR transitions, centred around the proton Larmor frequency, near $\nu_H \pm A_i/2$, were observed in the ENDOR spectrum. The transitions marked as A, B and C are high-frequency transitions (ν^+) with their pairing lines A*, B* and C* in the low-frequency region (ν^-). The two pairing lines at A* and B* are too weak to be observed and also further they are buried in the strong matrix lines. The pairing lines A* and B* are confirmed by the simulation. These anisotropic hyperfine coupling constants are assigned to the predominant hyperfine splitting arising from two equivalent protons, H_1 and H_4. The hyperfine tensor for protons at the 1 and 4 positions are of α-proton type with their principal component close to 0.5*a*, *a* and 1.5*a* along the C–H bond, along the normal to the benzene ring and perpendicular to the C–H bond, respectively. Here *a* is the isotropic hyperfine coupling constant. The α-proton type coupling is large in R–Ċ–H_a type radicals but in the present case, for the benzene radical cation, the hyperfine coupling is reduced due to delocalization

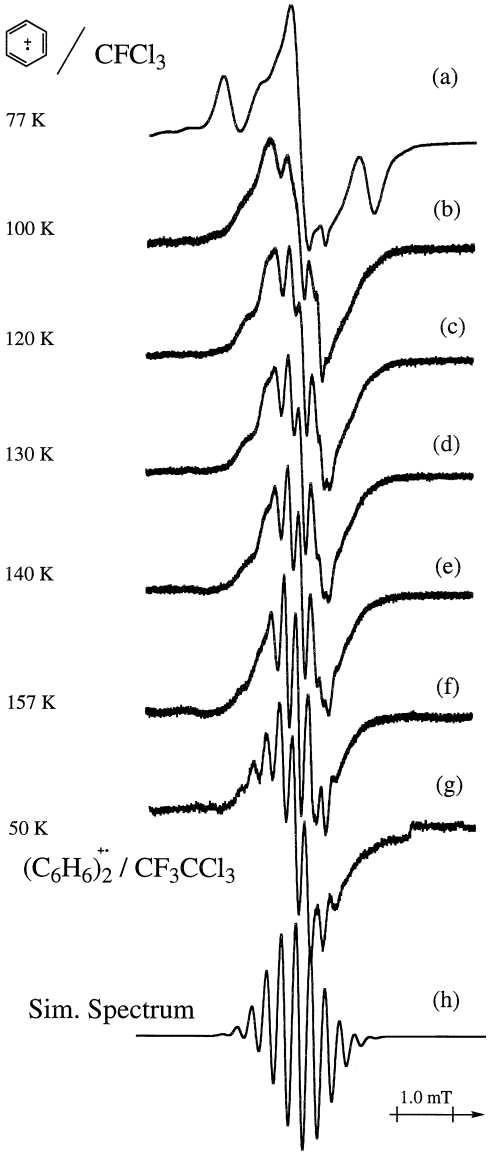

Fig. 2. EPR spectra of $C_6H_6^{+\cdot}$ in a $CFCl_3$ matrix at different temperatures (a–f) indicating the formation of $(C_6H_6)_2^{+\cdot}$. Figure includes the EPR spectrum of $(C_6H_6)_2^{+\cdot}$ in a CF_3CCl_3 matrix at 50 K (g) and the simulated spectrum of $(C_6H_6)_2^{+\cdot}$ (h).

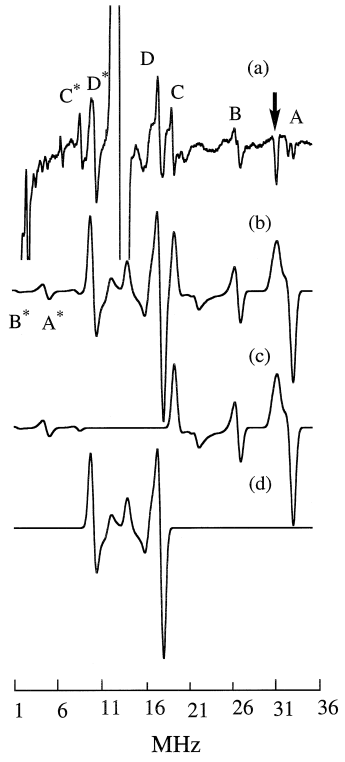

Fig. 3. Experimental (a) and simulated (b) powder ENDOR spectrum of $C_6H_6^{+\cdot}$ in a $CFCl_3$ matrix at 30 K. The arrow in the experimental spectrum indicates the ghost signal while recording the ENDOR spectrum. The intense line at 14 MHz and weaker lines in the 2–7 MHz region are due to the matrix and these lines are excluded in ENDOR simulation. Individual contributions arising from protons at the 1, 4 and the 2, 3, 5, 6 positions are shown in (c) and (d), respectively.

of the unpaired π-electron on the ring system. Consequently the ENDOR transitions are spread over a smaller frequency range allowing them to be detected even in a powder sample. The other set of transitions is marked as D and D*. The hyperfine tensor in this case is nearly axially symmetric. This smaller coupling is assigned to another set of four equivalent protons H_2, H_3, H_5 and H_6.

A series of simulations were performed with hyperfine parameters to fit both the EPR and ENDOR spectrum. We have excluded the matrix signal in the simulation. The ENDOR spectrum was simulated using an ENDOR simulation programme developed by Erickson [19] and is shown in Fig. 3 along with the experimental spectrum. The individual spectral contributions arising from the protons at the 1, 4 positions and those of the protons at the 2, 3, 5 and 6 positions are shown in Fig. 3c and d, respectively, to permit for proper assignment of the ENDOR transitions. It is seen from the experimental spectrum (Fig. 3a) that the ENDOR lines below ν_H are of lower intensity than the pairing lines above ν_H. This is attributed to the so-called hyperfine enhancement effect as reported earlier [20–22]. The deviation in the experimental ENDOR intensities from the calculated ones that was observed may be caused by relaxation and instrumental effects.

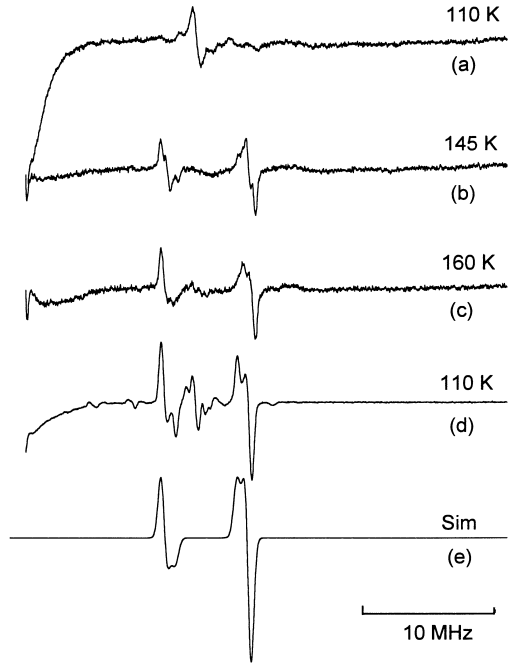

Fig. 4. The ENDOR spectra of $(C_6H_6)_2^{+\cdot}$ in a $CFCl_3$ matrix at different temperatures (a), (b) at 110, 145 K and (c) at 160 K. The ENDOR signal of $(C_6H_6)_2^{+\cdot}$ in a CF_3CCl_3 matrix at 110 K is shown in (d). The ENDOR simulated spectrum of $(C_6H_6)_2^{+\cdot}$ is shown in (e) for comparison. The ENDOR spectra were recorded by saturating the central EPR line of $(C_6H_6)_2^{+\cdot}$.

3.3. ENDOR results for $(C_6H_6)_2^{+\cdot}$

The ENDOR spectrum of the radical cation of the benzene dimer in the $CFCl_3$ matrix at 110 K showed a weak doublet centred around the proton Larmor frequency. The intensity of this signal increased with increasing temperature. At temperatures above 145 K, the orthorhombic spectrum changed to an axial spectrum. Beyond 160 K the signal disappeared completely due to melting of the matrix. The change of symmetry from orthorhombic to axial is probably due to dynamic averaging caused by rotation/pseudorotation of dimeric benzene about the six-fold axis giving an axial symmetry of hyperfine coupling. This is shown in Fig. 4a–c. The ENDOR spectrum of the $(C_6H_6)_2^{+\cdot}$ radical in the CF_3CCl_3 matrix showed axial symmetry throughout temperature range of observation and is also shown in Fig. 4d for comparison. We were unable to detect any ENDOR signal from the monomers at 100 K although it is present in the EPR spectrum. Note that the EPR signal could not be saturated at 100 K. The hyperfine tensors for $C_6H_6^{+\cdot}$ and $(C_6H_6)_2^{+\cdot}$ obtained from ENDOR data are given in Table 1.

4. Discussion

4.1. Monomeric benzene cation $C_6H_6^{+\cdot}$

Using $Q = 72.24$ MHz and the isotropic couplings for the two types of protons $a_1 = -25.31$ MHz and $a_2 = -5.43$ MHz, we have estimated the spin densities at the C_1 and C_2 carbon atoms from McConnell's relation $a_i = Q * \rho_i$ to be $\rho_1 = 0.35$ and $\rho_2 = 0.075$. The isotropic and the dipolar hyperfine coupling constants obtained in present investigations on the $C_6H_6^{+\cdot}$ radical cation in the $CFCl_3$ matrix are listed in Table 2 along with those obtained experimentally [7,8] and theoretically [15].

Table 2
Experimental and theoretical hyperfine data in MHz for $C_6H_6^{+\cdot}$

		This work	Ref. [7]	$^2b_{2g}$ Ref. [15]	$^2b_{1g}$ Ref. [15]	Ref. [8]
$H_{1i}H_4$	B_x	−13.50	−14.28	−15.96	+0.56	+0.90
	B_y	+14.22	+12.60	+18.76	+2.52	+0.90
	B_z	−0.70	+1.68	−2.80	−3.08	−1.68
	a	−25.31	−22.96	−26.88	+2.80	−12.24
$H_{2i}H_3$	B_1	−2.97	−3.36	−3.92	−11.48	+0.90
$H_{5i}H_6$	B_2	+5.43	+6.72	+7.00	+14.28	+0.90
	B_3	−2.46	−3.36	−2.80	−2.80	−1.76
	a	−5.43	−6.72	−3.92	−18.48	−12.24

B_i and a are the dipolar and isotropic hyperfine couplings obtained experimentally [7,8] and theoretically [15] compared to the results of this work. The data in this work, and Refs. [7] and [15] are for a rigid structure, and in Ref. [8] for $C_6H_6^{+\cdot}$ rotating about the six-fold axis (conversion factor is 1 G = 2.8024 MHz).

The dipolar couplings were also calculated by an extension of the method of McConnell and Strathdee, to include contributions from all carbon atoms carrying spin density as described previously [23]. The variation of the dipolar principal components with spin density was computed. By comparison with experimental values one obtains $\rho_1 = 0.34$, in agreement with the estimate based on the isotropic coupling. For the H_2, H_3, H_5 and H_6 protons nearly axial symmetry was predicted, in agreement with experiment. The calculation was done assuming that $\rho_2 = (1 - 2\rho_1)/4$.

The benzene radical cation with unpaired electron density in degenerate e_g orbital can undergo Jahn–Teller distortion with lifting of orbital degeneracy of the e_g orbital with unpaired electron density on either the $^2b_{2g}$ or $^2b_{1g}$ orbital. The experimental evidence obtained previously [7] and that obtained in the present ENDOR investigations suggest that the unpaired electron orbital has $^2b_{2g}$ character. The isotropic hyperfine coupling constants obtained from the ENDOR experiment for the two different types of protons, $a_1(2H) = -25.31$ MHz and $a_2(4H) = -5.43$ MHz, are close to those obtained by Iwasaki et al. ($a_1(2H) = -22.96$ MHz and $a_2(4H) = -6.72$ MHz) [7]. The hyperfine coupling constants obtained from configuration interaction calculations [15] among singly and doubly excited configurations of π-orbitals, −26.88 MHz (2H) and −3.92 MHz (4H), are also in good agreement but differ considerably for the $^2b_{1g}$ state, +2.80 MHz (2H) and −18.48 MHz (4H). This indicates that this state is not the one which is observed by ESR in halocarbon matrices. The recent experiments using high-resolution zero kinetic energy (ZEKE) threshold photoionization spectroscopy [24] of the benzene molecule gave direct evidence for the vibronic level terms in the distorted cation that are split by higher-order Jahn–Teller coupling between its $^2E_{1g}$ electronic ground state and the $\nu_6 e_{2g}$ in plane C–C–C ring bending vibrational mode. This is responsible for the Jahn–Teller distortion.

4.2. Dimeric benzene cation $(C_6H_6)_2^{+\cdot}$

The dimer radical cation is either sigma bonded as reported by Eberson et al. [25] or it can form a π-electron complex [16,17]. The σ-bonded benzene dimer complex can be easily distinguished from the π-electron complex, using both EPR and ENDOR spectroscopy. The σ-bonded benzene dimer complex is similar to the biphenyl radical cation and expected to give three sets of ENDOR transitions arising from the isotropic hyperfine interaction from the ortho, para and meta positions (a(para) = −17.70 MHz, a(ortho) = −8.87 MHz and a(meta) = −1.43 MHz) [11]. A pair of ENDOR transitions observed for the dimeric benzene radical cation in halocarbon matrices suggests a π-electron complex with a sandwich structure. This is further confirmed from computer simulation of the EPR and ENDOR spectrum.

4.3. Intermolecular distance in $(C_6H_6)_2^{+\cdot}$

The ENDOR spectra for the dimeric ion at 160 K in $CFCl_3$ and 110 K in CF_3CCl_3 showed that $|A_\perp|$

$> |A_{\|}|$, opposite to the case of the monomeric cation. In both cases, the effects of Jahn–Teller distortion had been thermally averaged to yield an even spin density, $\rho = 1/6$ in the monomeric ion, $1/12$ in the dimer and (pseudo)rotation about the six-fold axis gave axial symmetry of the hyperfine coupling. We attribute the result to the dipolar hyperfine interaction between the spin density on one benzene unit and the protons on the other. This provides a means to estimate the distance between the units, of the sandwich structure

$$A_{\|}^{\mathrm{mono}} = a + 2b, \tag{1}$$

$$A_{\|}^{\mathrm{di}} = a/2 + b + 2d, \tag{2}$$

$$d = \rho^{\mathrm{eff}} g_{\mathrm{N}} \beta_{\mathrm{N}} / r^3. \tag{3}$$

Here r is the distance between the units in Å, a and b are the isotropic and dipolar couplings for the monomer and d is the point dipolar hyperfine coupling between the spin density on the carbons of one unit and a proton on the other. The couplings are in gauss. From previous experimental data of the monomeric ion, $b = -0.63$ G and from the present results we obtain $d = 0.39$ G. Depending on the method used to evaluate ρ^{eff}, different values of r were calculated from Eq. (3). The limiting cases $\rho^{\mathrm{eff}} = 1/12$ (interaction with a single carbon atom) and $\rho^{\mathrm{eff}} = 1/2$ (interaction with all six carbon atoms) gave $1.82\,\text{Å} < r < 3.31\,\text{Å}$. To obtain a better estimate the differences in the H to C distances and the directions of the axes connecting them have to be considered. It is also of interest to investigate the geometry of other systems containing dimeric cations [18,25,26]. Work along these lines is in progress.

5. Conclusions

The ENDOR and EPR results obtained in the present investigations gave evidence for a Jahn–Teller distortion of the monomeric benzene radical cation $C_6H_6^{+\cdot}$ in a $CFCl_3$ matrix at 30 K, with unpaired electron density predominantly in the $^2b_{2g}$ orbital. The equivalence of the six protons is lost in this case, with the major spin density at protons at 1 and 4 compared to that of other protons. Better resolution in case of ENDOR spectroscopy compared to EPR enabled us to measure precisely the isotropic and dipolar hyperfine coupling constants in the Jahn–Teller distorted state of the two groups of protons, (H_1, H_4) and (H_2, H_3, H_5, H_6).

The ENDOR results of the dimeric benzene cation $(C_6H_6)_2^{+\cdot}$ formed from the monomer after warming in $CFCl_3$ and present in CF_3CCl_3 at all temperatures showed that the dimer had a sandwich structure in both matrices. The distance between the units was estimated with the help of the measured dipolar hyperfine couplings.

Acknowledgements

One of the authors (RMK) is thankful to the Department of Science and Technology (D.S.T.), India, for providing a Boyscast Fellowship. The author thanks Bhabha Atomic Research Centre (B.A.R.C.), India, for permitting him to work at the Department of Chemical Physics, Linköping University, Sweden.

References

[1] M.C.R. Symons, Chem. Soc. Rev. (1984) 393.
[2] M. Shiotani, Magn. Reson. Rev. 12 (1987) 333.
[3] A. Lund, M. Shiotani (Eds.), Radical Ionic Systems, Kluwer, Dordrecht, 1991.
[4] M. Iwasaki, K. Toriyama, K. Nunome, J. Am. Chem. Soc. 103 (1981) 3591.
[5] M. Iwasaki, K. Toriyama, K. Nunome, J. Chem. Soc. Chem. Commun. (1983) 202.
[6] K. Matsuura, K. Nunome, M. Okazaki, K. Toriyama, M. Iwasaki, J. Phys. Chem. 93 (1989) 6642.
[7] M. Iwasaki, K. Toriyama, K. Nunoma, J. Chem. Soc. Chem. Commun. (1983) 320.
[8] T. Komatsu, A. Lund, J. Phys. Chem. 76 (1972) 1727.
[9] R. Erickson, M. Lindgren, A. Lund, L. Sjöqvist, Collidal Surf. A 72 (1993) 207.
[10] R. Erickson, N.P. Benetis, A. Lund, M. Lindgren, J. Phys. Chem. A 101 (1997) 2390.
[11] R. Erickson, A. Lund, M. Lindgren, Chem. Phys. 193 (1995) 89.
[12] A. Volodin, V.A. Bolshov, G. Panov, J. Phys. Chem. 98 (1994) 7548.
[13] V.A. Bolshov, A.M. Volodin, G.M. Zhidomirov, A.A. Shubin, A. Bedilo, J. Phys. Chem. 98 (1994) 7551.
[14] E.A. Piocos, D.W. Werst, A.D. Trifunac, L.A. Eriksson, J. Phys. Chem. 100 (1996) 8408.

[15] M. Huang, S. Lunell, J. Chem. Phys. 92 (1990) 6081.
[16] O. Edlund, P.O. Kinell, A. Lund, A. Shimizu, J. Chem. Phys. 96 (1967) 3679.
[17] O. Edlund, P.O. Kinell, A. Lund, A. Shimizu, Adv. Chem. Ser. 82 (1968) 311.
[18] P.-O. Kinell, A. Lund, Acta Chem. Scand. 26 (1972) 444.
[19] R. Erickson, Chem. Phys. 202 (1996) 263.
[20] K. Toriyama, K. Nunome, M. Iwasaki, J. Chem. Phys. 64 (1976) 348.
[21] A. Schweier, Hs.H. Günthard, Chem. Phys. 70 (1982) 1.
[22] D.H. Whiffen, Mol. Phys. 10 (1966) 595.
[23] H.M. McConnell, J. Strathdee, Mol. Phys. 2 (1959) 129.
[24] R. Lindner, K. Müller-Dethlefs, E. Wedum, K. Haber, E.R. Grant, Science 271 (1996) 1698.
[25] L. Eberson, M.P. Hartshorn, O. Persson, J. Chem. Soc., Perkin Trans. 2 (1995) 409.
[26] O.W. Howarth, G.K. Fraenkel, J. Chem. Soc. 88 (1966) 4514.